Nitrogen and oxygen broadening of ozone infrared lines in 5mkm region: theoretical predictions by semiclassical and semiempirical methods

Jeanna Buldyreva, Nina Nikolaevna Lavrentieva

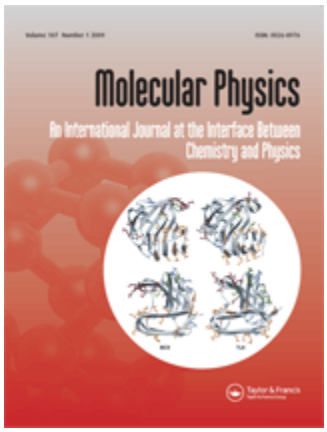

Nitrogen and oxygen broadening of ozone infrared lines in 5mkm region: theoretical predictions by semiclassical and semiempirical methods

Journal:	*Molecular Physics*
Manuscript ID:	TMPH-2009-0064.R1
Manuscript Type:	Full Paper
Date Submitted by the Author:	30-Mar-2009
Complete List of Authors:	Buldyreva, Jeanna; Université de Franche Comté, UTINAM Lavrentieva, Nina; Institute of Atmospheric Optics
Keywords:	Ozone, line width, infrared absorption, semiclassical calculation, semiempirical method
Note: The following files were submitted by the author for peer review, but cannot be converted to PDF. You must view these files (e.g. movies) online.	
MParticleO3_rev.tex New WinZip File.zip	

Nitrogen and oxygen broadening of ozone infrared lines in 5μm region: theoretical predictions by semiclassical and semiempirical methods

J. Buldyreva[a*] and N. Lavrentieva[b]

[a] Institut UTINAM, UMR CNRS 6213,Université de Franche-Comté,

16 route de Gray, 25030 Besançon cedex, France

[b] Institute of Atmospheric Optics, 1 Academicheskii av., 634055 Tomsk, Russia

Abstract

Pressure broadening coefficients of $\nu_1+\nu_3$ O_3-$N_2(O_2)$ vibrotational lines at room temperature are computed in the framework of the semiclassical formalism of Robert and Bonamy improved by exact trajectories and a semiempirical approach based on the Anderson theory. In the first method a more precise trajectory description enables a good (up to a few percent) **reproduction** of the experimental data available in the literature but is characterized by a quite high CPU cost. In the second method a simplified form of the scattering matrix accounts for the **subtle** effects of the trajectory curvature and vibrational dependence via effective adjustable parameters and noticeably reduces the CPU time without a loss of precision for further systematic computations. In contrast with the water molecule case, these parameters exhibit however a quite pronounced dependence on the rotational quantum number J values of lines used for fitting and should be properly adjusted for transitions from low, middle and high rotational levels.

Keywords: Ozone, line width, infrared absorption, pressure broadening, semiclassical calculation, semiempirical method

*Corresponding author. Email: jeanna.buldyreva@univ-fcomte.fr

1 Introduction

The spectral region of 5μm represents a particular interest for atmospheric spectroscopy of ozone since on these wavelengths the water absorption is extremely weak ("atmospheric window") and the most intense band $\nu_1 + \nu_3$ of the triad $2\nu_3/\nu_1 + \nu_3/2\nu_1$ is located. This region has been therefore quite intensively studied experimentally (see e.g. [1, 2, 3]) and advanced **semiclassical** computations [2, 4] have been made. The reliable retrieval of concentration and temperature vertical O_3 profiles from these spectra is however conditioned by a precise knowledge of the individual line parameters: position, intensity, pressure-broadened half width, pressure-induced line shift and their temperature dependences. **For** the line **widths** the required precision is estimated to be about 2% whereas actually it often reaches 10% for experiments as well as for computations.

The present work revisits theoretically the room-temperature ozone line broadening by nitrogen and oxygen aiming to improve the agreement with experimental values [2, 3]. Two theoretical approaches are tested: the semiclassical formalism of Robert and Bonamy improved by exact isotropic trajectories (RBE) [5] and **a semiempirical (SE) model [6] inspired by the Anderson theory**. The first approach **allows to assess the importance of** the trajectory model via a comparison with the **results** of Bouazza et al. [2] based on the **parabolic-trajectory** Robert and Bonamy formalism **for asymmetric tops** [7]. The second approach yields a rapid estimation of asymmetric-top line broadening coefficients without a noticeable loss of precision owing to preliminary fitted empirical parameters taking into account the trajectory curvature, the corrections to the scattering matrix and the vibrational effects.

The following section gives a brief description of both theoretical approaches with specification for O_3-$N_2(O_2)$ case. A detailed analysis of the dependence of the broadening coefficients on various quantum numbers is presented and discussed in Section 3. The concluding remarks are summarized in the final section.

2 Theoretical background

2.1 Semiclassical approach

According to the RBE formalism extended to the case of asymmetric rotors [5], the basic expression [8] for the half-width at half-height (HWHH) of a vibrotational[1] line corresponding to the optical transition $f \leftarrow i$ (in cm^{-1})

$$\gamma_{fi} = \frac{n}{2\pi c}\langle v\{1-(1-S^L_{2,f2i2})e^{-\left[S_{2,i2}+S_{2,f2}+S^C_{2,f2i2}\right]}\}\,\rangle_{b,v,\{2\}} \tag{1}$$

(n is the number density of perturbing particles in the states characterized by the set of quantum numbers $\{2\}$, c is the speed of light, v is the relative velocity and b is the impact parameter replaced further by the distance of the closest approach r_c) involves **the real parts**[2] of the second-order contributions $S_{2,i}$, $S_{2,f}$, $S^C_{2,f2i2} = \sum_{J'_2=J_2} S_{2,f2'i2'}$, $S^L_{2,f2i2} = \sum_{J'_2\neq J_2} S_{2,f2'i2'}$ which are no more given by analytical formulae. Indeed, the rotational wave functions of asymmetric top $|J\tau M\rangle$ ($|JK_aK_cM\rangle$ in alternative notation) are expressed as a linear combination of the wave functions of symmetric top $|JKM\rangle$:

$$|J\tau M\rangle = \sum_K a_K^{J\tau}\,|JKM\rangle\,, \tag{2}$$

where $K = -J, -J+1, ..., 0, J-1, J$. Moreover, the rotationally invariant expansion [9] of the interaction potential between the active (1) and perturbing (2) molecules

$$V(\vec{r}) = \sum_{l_1l_2l}\sum_{k_1k_2} V^{k_1k_2}_{l_1l_2l}(r) \sum_{m_1m_2m} C^{lm}_{l_1m_1l_2m_2} D^{l_1}_{m_1k_1}(\Omega_1)^* D^{l_2}_{m_2k_2}(\Omega_2)^* Y_{lm}(\Omega)^* \tag{3}$$

over the rotational Wigner matrices $D^{l_x}_{m_xk_x}(\Omega_x)$, x=1,2 (related to the orientations of the principle molecular axes of two interacting molecules in the laboratory fixed frame) and the spherical harmonic $Y_{lm}(\Omega)$ (tied to the intermolecular distance vector $\vec{r}$ orientation in the same frame) contains the radial components which **depend** on the projections k_1, k_2 on the molecular axes. (The asterisk in Eq. (3) and below stands for complex conjugation.)

[1]The dependence on vibrational quantum numbers is omitted in the following since both isotropic and anisotropic parts of the available interaction potential are vibrationally independent; **the first-order terms proportional to the vibrational matrix elements of the isotropic potential do not appear therefore in the line width expression.** This dependence is however tacitly accounted for through the O_3 energy levels and coefficients of the rotational wave functions in the final state.

[2]**The noncommutative character of the interaction at two different instants is neglected, so that the imaginary part of the second-order contributions vanishes.**

For the collision of an asymmetric active molecule with a linear perturbing molecule ($k_2 = K_2 = K_2' = 0$) which occurs in the XOY plane, the second-order contributions read [5]

$$S_{2,i2} = \frac{2r_c^2}{\hbar^2 v^2} \sum_{J_i'\tau_i' J_2'} \sum_{l_1 l_2 l} \frac{(C^{J_2'0}_{J_2 0 l_2 0})^2}{(2l_1+1)(2l_2+1)} \sum_m \frac{(l-m)!(l+m)!}{2^{2l}((l-m)/2)!^2((l+m)/2)!^2} \times \left| \sum_{k_1} (-1)^{k_1} X^{l_1}_{-k_1}(J_i \tau_i J_i' \tau_i') \mathcal{I}^{k_1 0}_{l_1 l_2 l m}(\omega_{i2,i'2'}) \right|^2 , \quad (4)$$

$$S_{2,f2'i2'} = -\frac{4r_c^2(-1)^{J_i+J_f+J_2+J_2'+\rho}}{\hbar^2 v^2} \sqrt{(2J_i+1)(2J_f+1)} \times \sum_{l_1 l_2 l} \frac{(-1)^l W(J_i J_f J_i J_f; \rho l_1)}{(2l_1+1)(2l_2+1)} (C^{J_2'0}_{J_2 0 l_2 0})^2 \sum_m \frac{(l-m)!(l+m)!}{2^{2l}((l-m)/2)!^2((l+m)/2)!^2} \times \left[\sum_{k_1} (-1)^{k_1} X^{l_1}_{-k_1}(J_f \tau_f J_f \tau_f) \mathcal{I}^{k_1 0}_{l_1 l_2 l m}(\omega_{2'2}) \right] \times \left[\sum_{\eta_1} (-1)^{\eta_1} X^{l_1}_{-\eta_1}(J_i \tau_i J_i \tau_i) \mathcal{I}^{\eta_1 0}_{l_1 l_2 l m}(\omega_{22'}) \right] , \quad (5)$$

where the notation

$$X^{l_1}_{k_1}(J_i \tau_i J_i' \tau_i') \equiv \sum_{K_i K_i'} a^{J_i \tau_i *}_{K_i} a^{J_i' \tau_i'}_{K_i'} C^{J_i' K_i'}_{J_i K_i l_1 k_1} \quad (6)$$

is used, and the trajectory integrals (in terms of the dimensionless variable $y = r/r_c$ and the resonance parameter $k_c = \omega r_c / v$)

$$\mathcal{I}^{k_1 0}_{l_1 l_2 l m}(\omega) \equiv \int_1^\infty \frac{dy y \tilde{V}^{k_1 0}_{l_1 l_2 l}(y r_c) \cos\left[k_c A_0(y) - m\sqrt{1 - V^\star_{iso}(r_c)} A_2(y)\right]}{\sqrt{y^2 - 1 + V^\star_{iso}(r_c) - y^2 V^\star_{iso}(y r_c)}}, \quad (7)$$

$$A_n(y) = \int_1^y \frac{dz}{z^{n-1}\sqrt{z^2 - 1 + V^\star_{iso}(r_c) - z^2 V^\star_{iso}(z r_c)}} \quad (8)$$

depend on the radial anisotropic potential components $\tilde{V}^{k_1 0}_{l_1 l_2 l} = [(2l+1)/(4\pi)]^{1/2} V^{k_1 0}_{l_1 l_2 l}$, the reduced value of the isotropic potential $V^\star_{iso} = 2V_{iso}/(m^\star v^2)$ ($m^\star$ is the reduced mass of the molecular pair) and the frequencies $\omega_{i2,i'2'} = \omega_{ii'} + \omega_{22'}$ where $\omega_{ii'}$ and $\omega_{22'}$ correspond to the transitions induced by the collision in the active and perturbing molecules; $W(J_i J_f J_i J_f; \rho l_1)$ is a Racah coefficient. **For the perturbing molecule only the thermally populated rotational levels J_2 of the ground vibrational state are traditionally considered.**

The trajectory integrals $\mathcal{I}^{k_1 0}_{l_1 l_2 l m}$ can not be summed **analytically** on m **to yield resonance functions as in** the case of two linear molecules, so they are precomputed by a

numerical integration procedure for various r_c, k_c and T values, and further injected in the line-width calculation code. **The mean thermal velocity is used instead of averaging with the Maxwell-Boltzmann distribution of velocities.** The collision-induced frequencies for the perturbing molecules $\omega_{22'}$ can be easily calculated with the corresponding values of rotational constants $B_0(N_2)$=1.989622 cm^{-1} [10] and $B_0(O_2)$=1.4377 cm^{-1} deduced from B_e and α_e of Herzberg [11]. In contrast, the frequencies $\omega_{ii'}$ for the active ozone molecule are more difficult to obtain.

2.1.1 O_3 energy levels and wave functions

Like any asymmetric top, the rotational energy levels of ozone molecule can not be represented by an analytical formula. Only approximate expressions or a numerical diagonalisation of the rotational Hamiltonian can be used. For the excited vibrational states, the vibrational symmetry should **also be** accounted for, so that diagonalisation **has to be performed** for the rotational structure of each vibrational level involved in the considered vibrotational transition. For the spectral lines of the $\nu_1+\nu_3$ band the energy levels of the ground (000) and the excited (101) states are thus needed. They were taken directly from the IAO ozone database [12] for the ground state and were kindly provided by S. Michajlenko for the triad (002)/(200)/(101) [13].

The expansion coefficients $a_K^{J\tau}$ in Eq. (2) are obtained together with the rotational energies by a numerical diagonalisation of the rotational Hamiltonian. This diagonalisation is however **easier to perform** within a symmetrized symmetric-top basis $|J\mathcal{K}\gamma\rangle$ ($\mathcal{K}=0,...,J$, $\gamma=\pm1$):

$$|J\mathcal{K}\gamma\rangle = \frac{1}{\sqrt{2}}(|JK\rangle + \gamma\,|J\ -K\rangle). \tag{9}$$

The corresponding expansion of the asymmetric-top wave function reads

$$|J\tau\rangle = \sum_{\mathcal{K}} C_{\mathcal{K}}^{J}\,|J\mathcal{K}\gamma\rangle\,. \tag{10}$$

Substitution of Eq. (9) into Eq. (10) and comparison with Eq. (2) yield the relations between the expansion coefficients for $\mathcal{K}=1,...,J$:

$$a_K^{J\tau} = C_{\mathcal{K}}^{J}/\sqrt{2},\ a_{-K}^{J\tau} = \gamma C_{\mathcal{K}}^{J}/\sqrt{2}, \tag{11}$$

and $a_0^{J\tau} = C_0^J$ for $K=\mathcal{K}=0$, $\gamma=1$.

The coefficients $C_{\mathcal{K}}^{J}$ for the ground (000) and excited (101) states were **provided** together with the O_3 vibrotational energy levels [12, 13] and correspond to the molecular frame shown in Figure 1. To identify the J, $\mathcal{K}$ and γ values corresponding to non

zero coefficients, Tables 5.4-5.5 for the ground state and Tables 5.4, 5.8 for the excited state from Ref. [14] were used. **The excited (101) vibrational state interacts with (002) and (200) states, and the corresponding vibrotational wave functions contain the $C^J_{\mathcal{K}}$ coefficients describing the mixing effects. However, for the considered vibrotational levels these mixing coefficients are small, and after additional testing we retained in our computation only the coefficients relative to (101) state.** The expansion coefficients $a^{J\tau}_K$ **were** further easily obtained by Eq. (11). **To reduce** CPU time the functions $X^{l_1}_{k_1}$ of Eq. (6) containing these coefficients **were precomputed** for the given pairs of levels $(J_i\tau_i)$, $(J'_i\tau'_i)$ and given l_1, k_1.

2.1.2 Interaction potential

Like for the majority of polyatomic molecules, **the interaction potential energy of the asymmetric top O_3 with perturbing particles is out of reach of current** quantum-mechanical *ab initio* calculations. This interaction energy for O_3-$N_2(O_2)$ is therefore approximated [2, 4, 15] by a sum of the leading electrostatic components (dipole-quadrupole plus quadrupole-quadrupole interactions) and atom-atom contributions of Lennard-Jones form:

$$V = V^{el} + V^{aa} = V_{\mu_1 Q_2} + V_{Q_1 Q_2} + \sum_{i,j} \left(\frac{d_{ij}}{r^{12}_{1i,2j}} - \frac{e_{ij}}{r^{6}_{1i,2j}} \right), \tag{12}$$

where the subscripts 1 and 2 refer respectively to the active (O_3) and perturbing (N_2 or O_2) molecules. The interatomic parameters $d_{ij} = 4\varepsilon_{ij}\sigma^{12}_{ij}$ and $e_{ij} = 4\varepsilon_{ij}\sigma^{6}_{ij}$ are defined directly by the Lennard-Jones parameters ε_{ii}, σ_{ii} for homonuclear atom-atom interactions and are constructed by the combination rules [16] $\varepsilon_{ij} = (\varepsilon_{ii}\varepsilon_{jj})^{1/2}$, $\sigma_{ij} = (\sigma_{ii} + \sigma_{jj})/2$ for heteronuclear atom-atom interactions.

The interaction potential has to be cast into the particular form of Eq. (3). The radial potential components $V^{k_1 0}_{l_1 l_2 l}(r)$ appear then as [5]

$$\begin{aligned} V^{k_1 0}_{l_1 l_2 l}(r) &= A_{l_1 l_2} \frac{\Theta_{l_1 k_1} \Theta_{l_2 0}}{r^{l+1}} \\ &+ \sum_{ij} \left[d_{ij} f^{12}_{l_1 l_2 l}(r_{1i}, r_{2j}, r) - e_{ij} f^{6}_{l_1 l_2 l}(r_{1i}, r_{2j}, r) \right] Y_{l_1 k_1}(\Omega'_{1i}) Y_{l_2 0}(\Omega'_{2j}) \end{aligned} \tag{13}$$

where the coefficients $A_{l_1 l_2}$ are given by [9]

$$A_{l_1 l_2} = \frac{(-1)^{l_2}}{2l+1} \left[\frac{(4\pi)^3 (2l+1)!}{(2l_1+1)!\,(2l_2+1)!} \right]^{1/2}, \tag{14}$$

$\Theta_{l_x k_x}$ represent the spherical multipole components in the molecular fixed frame and the functions $f^n_{l_1 l_2 l}$ come from the two-center expansion of $r^{-n}_{1i,2j}$ [17]:

$$f^n_{l_1 l_2 l}(r_{1i}, r_{2j}, r) \equiv \frac{(-1)^{l_2}}{r^n}\left[\frac{(4\pi)^3\,(2l_1+1)\,(2l_2+1)}{(2l+1)}\right]^{1/2} C^{l0}_{l_1 0 l_2 0} \times \sum_{p,q}\left(\frac{r_{1i}}{r}\right)^p \left(\frac{r_{2j}}{r}\right)^q \frac{(n+p+q-l-3)!!\,(n+p+q+l-2)!!}{(n-2)!\,(p-l_1)!!\,(p+l_1+1)!!\,(q-l_2)!!\,(q+l_2+1)!!} \times \{1+\delta_{n1}(\delta_{pl_1}\delta_{ql_2}\delta_{p+q,l}-1)\}\ , \tag{15}$$

$p = l_1, l_1+2, l_1+4, \ldots$ and $q = l_2, l_2+2, l_2+4, \ldots$. To compute these radial components one needs to precise the orientation of each atom in the molecular fixed frame. For the O_3 molecular frame defined in Fig. 1 the spherical harmonics $Y_{l_1 k_1}(\Omega'_{1i})$ have only real components; for the linear perturbing molecule N_2 (O_2) the molecular axis is taken to be the z-axis. For such a choice of molecular frames the multipole components are given in Table 1 and the non-vanishing radial potential components are listed in Appendix. The isotropic part of the interaction potential is traditionally taken in Lennard-Jones form with the parameters $\varepsilon = 150\ K$, $\sigma = 3.93\ \mathring{A}$ (O_3-N_2) and $\varepsilon = 174\ K$, $\sigma = 3.77\ \mathring{A}$ (O_3-O_2) [2].

2.1.3 Selection rules for collision-induced transitions

Molecular collisions induce only purely rotational transitions within the same vibrational level, i.e. for the active molecule there are $J_i \rightarrow J'_i$ transitions within the ground vibrational state and $J_f \rightarrow J'_f$ transitions within the vibrationally excited (101) state; for the perturbing molecule only the rotational transitions within the ground state occur. According to Eq. (6), the collision-induced transitions in the active molecule are determined by the Clebsch-Gordan coefficient $C^{J'_i K'_i}_{J_i K_i l_1 k_1}$ which needs $J_i - l_1 < J'_i < J_i + l_1$ and $K'_i = K_i + k_1$. Since these transitions are purely rotational, they should obey the additional selection rules for the allowed changes of $K_a + K_c$ [18]: for $J + \tau$ even $\Delta(K_a + K_c) = 1, 2$ for R-branch, $\Delta(K_a + K_c) = -1, 0$ for P-branch and $\Delta(K_a + K_c) = 0, 1$ for Q-branch, whereas for $J + \tau$ odd $\Delta(K_a + K_c) = 1, 0$ for R-branch, $\Delta(K_a + K_c) = -1, -2$ for P-branch and $\Delta(K_a + K_c) = 0, -1$ for Q-branch. For the perturbing linear and centrosymmetric molecule l_2 can take only even values. The Clebsch-Gordan coefficients $C^{J'_2 0}_{J_2 0 l_2 0}$ are therefore non vanishing for $J_2 + J'_2$ even, and the collisional transitions takes place for $J'_2 = J_2 - l_2, ..., J_2 + l_2$.

2.2 Semiempirical approach

Despite the numerous drawbacks (interactions limited to long-range forces, straight-line trajectories, awkward cutoff procedure) the impact approach developed by Anderson, Tsao and Curnutte [19, 20] (Anderson or ATC theory) has an important advantage of simplicity and clear physical meaning. This advantage becomes crucial when complete infrared absorption spectra of polar polyatomic molecules (H_2O, O_3, ...) composed of thousands of lines are to be calculated. For this kind of situation the fine details of collisions and intramolecular dynamics accounted for by the semiclassical approach of Robert and Bonamy (in its **original** "parabolic-trajectory" **form** [7, 21] with tedious analytical expressions or in the "exact-trajectory" improvement [5] with numerical integration on trajectories) lead to very time-consuming calculations. It is therefore very worthy to modify the precise semiclassical approach in order to decrease the computational effort without loss of precision. Such a modification can be made by transforming the general RB equations into a simpler ATC form **while simultaneously** introducing fitting parameters **to** account for the corrections to the scattering matrix, trajectory curvature and vibrational effects. Determination of these parameters can benefit from an extensive use of empirical data **available** for various vibrational bands. This semiempirical approach was proposed in [6] and resulted in accurate predictions of line shape parameters and their temperature dependences for H_2O-$N_2(O_2)$ and CO_2-$N_2(O_2)$ colliding systems [22, 23, 24]. The results of these calculations have been included in a freely-available carbon dioxide spectroscopic data bank [25] and in the "ATMOS" Information System [26]. Recently this method has been further developed by using anharmonic wave functions for the estimation of line shape parameters for H_2O-$N_2(O_2, H_2O)$ colliding systems and resulted in a much better agreement of calculated line widths and shifts with their observed values [27, 28, 29, 30]. **Given the very satisfactory results obtained for H_2O, it is worth to apply this method to the asymmetric top O_3 in order to facilitate the line width calculations for this important atmospheric molecule and provide extensive theoretical data for molecular databases.**

According to the ATC theory the semiclassical line width depends on the transition probabilities[3] $D^2(ii'|l)$ and $D^2(ff'|l)$ of the different scattering channels $i \to i'$, $f \to f'$ **which are defined only by** the properties of the active molecule (intramolecular

[3]**These transition probabilities represent the squared reduced matrix elements of the relevant molecular operators of different tensor types: dipole (l=1), quadrupole (l=2), etc.**

effects) and can be considered as very well known quantities. The line width expression can be expanded **therefore** into a series over these transition probabilities:

$$\gamma_{fi} = A(i,f) + \sum_{l,i'} D^2(ii'|l) P_l(\omega_{ii'}) + \sum_{l,f'} D^2(ff'|l) P_l(\omega_{ff'}) + ... \tag{16}$$

(higher order terms are neglected), giving thus an expression similar to that of Anderson theory. The first term of Eq.(16) is a usual ATC term issued from the cutoff procedure with the interruption radius $b_0(i, f, J_2, v)$. The expansion coefficients $P_l(\omega_{ii'})$, called "interruption" or "efficiency functions" for a given scattering channel, depend on the properties of the absorbing molecule, the intermolecular potential, the trajectory, the energy levels and the wave functions of the perturbing molecule. They are not known with a high accuracy, and the semiempirical approach consists in their refinement by means of an adjustable correction factor:

$$P_l(\omega) = P_l^A(\omega) C_l(\omega) \ , \tag{17}$$

where $P_l^A(\omega)$ is the interruption function of the Anderson theory and $C_l(\omega)$ is obtained by fitting of computed line widths to experimental data. The factor $C_l(\omega)$ **takes into account the rotational dependence of the interruption function**[4] **which is modelled by [6]:**

$$C_l(\omega) = \frac{c_1}{c_2\sqrt{J}+1} \tag{18}$$

and has typically a small value. When this rotational dependence is realistic (for example, for the water vapor active molecule), the fitting parameters c_1 and c_2 are responsible, respectively, for the correction of the error induced by the cutoff procedure and the vibrational dependence. In this case, if the experimental values used for fitting are accurate, any two experimental values should be in principle sufficient to obtain reliable values of c_1 and c_2 parameters for all the lines of the considered vibrational band. Moreover, since the line widths depend only slightly on vibrational quantum numbers (maximal difference of a few percent), c_1 and c_2 values obtained for one vibrational band can be quite surely used for other bands. This fact has been already confirmed for H_2O-$N_2(O_2)$ and CO_2-$N_2(O_2)$ molecular systems [22, 23, 24], for which c_1 and c_2 parameters fitted to few values of broadening coefficients in a given vibrational band describe correctly not only all the experimental data in this band but also the whole variety of bands for the colliding molecular pair.

[4]The interactions involving the dipole moment of the active molecule are supposed to be dominant, so that only one pair of c_1, c_2 parameters corresponding to $l = 1$ is considered.

The second and third terms of Eq (16) dependent on the transition probabilities correspond to the second-order contributions with respect to the interaction potential:

$$S_2 = S_2^{12e} + S_2^{22e} + S_2^{22p} + S_2^{02p} + S_2^{20p} \ , \tag{19}$$

where the superscripts 1 and 2 stand for the tensorial order of the multipole interactions (12 - dipole-quadrupole interaction, 22 - quadrupole-quadrupole interaction, etc.) and the superscripts e and p mean the electrostatic and the polarisation parts of the interaction potential (detailed expressions of these terms can be found in [20, 31]). For the active ozone molecule it should be additionally kept in mind that its dipole moment is small (0.53D) whereas the mean dipole polarizability is quite high (2.8 $\overset{\circ}{A}^3$). The polarization terms S_2^{22p}, S_2^{02p}, S_2^{20p} are expected therefore to be significant.

3 Results and discussion

Line width calculations by both theoretical approaches were realized for P-, Q- and R-branches of $\nu_1 + \nu_3$ vibrational band of O_3-N_2 and O_3-O_2 systems at room temperature (297 K). We considered the transitions for which experimental data [2, 3] and traditional RB computations with parabolic trajectories [2] are available.

In the framework of the semiempirical approach the energy levels and wave functions were calculated with the effective Hamiltonian of Watson without taking into account Coriolis and Darling-Dennison resonances. Indeed, from direct calculations it was found that omitting accidental resonances does not result in significant errors in the calculation of line widths. The rotational and centrifugal distortion constants of the ground and excited vibrational states of the active molecule were taken from [32]. Since the calculations mainly concerned high values of the rotational quantum number J, we took into account many scattering channels induced by collisions and allowed by the symmetry (many more than for low values of J). In order to increase the number of the scattering channels contributions in calculation we estimated the contributions of corresponding channels to the line broadening and then sorted them. It was found in particular that the contributions from scattering channels with $\omega_{ii'}$ >700 cm^{-1} and $K_a - K'_a$ >3 are negligible.

Figure 2 shows our results together with measurements and **RB**-calculations of Refs [2, 3] for the case of Q-branch where the small number of observed transitions facilitates the comparison. For the horizontal axis we have chosen a specific representation with the J-value incremented by 0.1 of K_a value in order to separate the line widths with the same

J but different K_a values. As can be seen from this figure, for both perturbing molecules the use of exact trajectories in the semiclassical approach **improves** the agreement with experiment. **It should be noted however that while the potential energy surfaces, the relative velocity (mean thermal velocity) and the perturber states were exactly the same in both RB and RBE approaches, the vibrotational wave functions and the O_3 energy levels were taken from different sources which might have some influence on the results.** The efficiency of the semiempirical approach intended for rapid prediction of broadening coefficients for line manifolds is much better visualized on Fig. 3 **where an example of O_3-N_2 P-branch transitions is presented** (for R-**branch and** O_3-O_2 system the situation is quite similar). On this figure again the term $0.05(K_a\text{-}1)$ added to the usual abscisse J allows separation of results belonging to the transitions with identical J but different K_a quantum numbers. To fit the parameters c_1, c_2 experimental points were chosen in both branches with arbitrary J-values, leading to $c_1 = 2.7$ and $c_2 = 7.0$. The crosses corresponding to the semiempirical line widths are clearly closer to the experimental values than the theoretical RB predictions (RBE results are not shown on this figure for the sake of clarity).

In contrast with the case of H_2O active molecule where the adjustable parameters c_1 and c_2 keep (practically) the same values when fitted to various (small, middle, high) J transitions and in different branches of the same vibrational band, for the ozone broadening coefficients these parameters show a quite pronounced dependence on the J-range.[5] As can be seen on Fig. 4a for P- and R-branches of O_3-N_2 system, when the parameters are obtained by fitting to some experimental line widths from both branches but with high J-values only (crosses), their values $c_1 = 3.0$ and $c_2 = 0.2$ lead to too small broadening coefficients for low-J transitions. When the fitting and calculation are made separately for low **($3 \leq J \leq 16$)**, middle **($17 \leq J \leq 23$)** and high **($24 \leq J \leq 41$)** J-value regions, the pairs of parameters reproduce the measurements quite well. It can be stated however that for high rotational quantum numbers both parameters differ significantly from their values for low and middle J: c_1 equals 2.9 instead of 2.5-2.6 and c_2 decreases from 7.0-6.8 by a factor of 2. For O_3-O_2 system (Fig. 4b) a direct fitting to small, middle and high J transitions **gives** c_1, c_2 values about one order of magnitude greater than for O_3-N_2 case, with the c_2 parameter value significantly higher for low J than for middle and high J.

[5] **An additional test realized with a separate fitting for P- and R-branches resulted in approximately the same quality of c_1, c_2 parameters and in a very slight improvement of theoretical values, so that its results are not presented here.**

This strong variation of c_2 **hints** that the correction factor of Eq. (18) should be improved for a better modelling of rotational dependence at high J values. **Indeed, the observed dependence of c_1, c_2 parameters on J-value region can be attributed to the small dipole moment of O_3 and a possible variation of the correction factors $C_l(\omega)$ for $l \geq 2$. In other words, one pair of c_1, c_2 parameters (corresponding to the dominant contribution $l = 1$ for H_2O) is no more sufficient to correctly describe the line widths, and at least one additional pair (corresponding to $l = 2$) should be included in the fitting procedure. The choice of fitting parameters for O_3-$N_2(O_2)$ systems deserves therefore a more detailed study.**

For a more exhaustive analysis of the rotational J-dependence of the considered line widths, we have also studied this dependence for some "families" of lines. Figure 5 gives two examples for the R-branch of O_3-N_2 system. For these lines the semiclassical approaches RB and RBE demonstrate a similar quality of results whereas the simple semiempirical approach proves again its efficiency.

Finally, we have looked for the K_a-dependence of the lines with the same J value. As can be seen on Fig. 6 for O_3-N_2 R-branch, the experimentally observed increase and then a slight decrease of line broadening coefficient with increasing K_a values are in general correctly predicted by both SE and RBE approaches. (Missing RB-values for $J = 4$, $K_a = 4$ and $J = 24$, $K_a = 8$ do not allow to conclude on the efficiency of this method.) More experimental results are however desirable for a more exhaustive study of this dependence.

4 Conclusions

In the present paper we have theoretically studied N_2- and O_2-pressure broadening coefficients for $\nu_1 + \nu_3$ vibrotational lines of ozone. Our first semiclassical approach has demonstrated the **efficiency** of exact trajectories **to describe experimental data**. Its **use** required in particular theoretical expressions for the interaction potential radial components corresponding to the molecular frame of ozone molecule for which its rotational wave functions are available. However, the CPU cost of this method being quite high, a simplified semiempirical approach has been also attempted, which allowed to describe **quite** easily and successfully all the manifold of lines with the help of some adjustable parameters accounting for the trajectory curvature, corrections to the scattering matrix and vibrational effects. In contrast with the very polar water molecule, for the strongly

polarizable ozone active molecule these parameters had to be adjusted separetely for low, middle and high values of the rotational quantum number J in order to correct the usually chosen rotational dependence of the correction factor. **The possible variation of correction factors for $l \geq 2$ and the necessity of more exhaustive studies to draw a definit conclusion on this point have been evoked.** Since the vibrational dependence of line widths is known to be weak, the obtained values of adjustable parameters can be used for theoretical estimation of broadening coefficients in other vibrational bands of ozone **which represents a great interest for molecular databases**.

Acknowledgements

The authors acknowledge the financial support by the French national program *Les Enveloppes Fluides et l'Environnement – CHimie ATmosphérique (LEFE-CHAT)* and by RAS program "Optical spectroscopy and Frequency Standards".

Appendix

Non-vanishing radial components of the interaction potential O_3-N_2 as defined by the O_3 molecular frame of Fig. 1:

$$
\begin{aligned}
V^{00}_{022}(r) &= \frac{4\sqrt{5\pi}}{r^6}\left\{\frac{d_{ON}}{r^6}\left[\Xi^{12}_{022}(O_1)+2\Xi^{12}_{022}(O_2)\right]-e_{ON}\left[\Xi^{6}_{022}(O_1)+2\Xi^{6}_{022}(O_2)\right]\right\}\\
V^{\pm 10}_{101}(r) &= \mp\frac{2\sqrt{3\pi}}{r^6}\left\{\frac{d_{ON}}{r^6}\left[\Xi^{12}_{101}(O_1)+0.4022\Xi^{12}_{101}(O_2)\right]-e_{ON}\left[\Xi^{6}_{101}(O_1)+0.4022\Xi^{6}_{101}(O_2)\right]\right\}\\
V^{\pm 10}_{121}(r) &= \pm\frac{4\sqrt{15\pi}}{r^6}\left\{\frac{d_{ON}}{r^6}\left[\Xi^{12}_{121}(O_1)+0.4022\Xi^{12}_{121}(O_2)\right]-e_{ON}\left[\Xi^{6}_{121}(O_1)+0.4022\Xi^{6}_{121}(O_2)\right]\right\}\\
V^{\pm 10}_{123}(r) &= \mp\frac{\sqrt{30\pi}}{\sqrt{7}r^4}\mu_x^{O_3}Q_{zz}^{N_2}\\
&\mp \frac{6\sqrt{30\pi}}{\sqrt{7}r^6}\left\{\frac{d_{ON}}{r^6}\left[\Xi^{12}_{123}(O_1)+0.4022\Xi^{12}_{123}(O_2)\right]-e_{ON}\left[\Xi^{6}_{123}(O_1)+0.4022\Xi^{6}_{123}(O_2)\right]\right\}\\
V^{00}_{202}(r) &= -\frac{2\sqrt{5\pi}}{r^6}\left\{\frac{d_{ON}}{r^6}\left[\Xi^{12}_{202}(O_1)-3.7574\Xi^{12}_{202}(O_2)\right]-e_{ON}\left[\Xi^{6}_{202}(O_1)-3.7574\Xi^{6}_{202}(O_2)\right]\right\}\\
V^{\pm 20}_{202}(r) &= \frac{\sqrt{30\pi}}{r^6}\left\{\frac{d_{ON}}{r^6}\left[\Xi^{12}_{202}(O_1)+0.0808\Xi^{12}_{202}(O_1)\right]-e_{ON}\left[\Xi^{6}_{202}(O_1)+0.0808\Xi^{6}_{202}(O_2)\right]\right\}\\
V^{00}_{220}(r) &= -\frac{10\sqrt{5\pi}}{r^6}\left\{\frac{d_{ON}}{r^6}\left[\Xi^{12}_{220}(O_1)-3.7574\Xi^{12}_{220}(O_2)\right]-e_{ON}\left[\Xi^{6}_{220}(O_1)-3.7574\Xi^{6}_{220}(O_2)\right]\right\}\\
V^{\pm 20}_{220}(r) &= \frac{5\sqrt{30\pi}}{r^6}\left\{\frac{d_{ON}}{r^6}\left[\Xi^{12}_{220}(O_1)+0.0808\Xi^{12}_{220}(O_2)\right]-e_{ON}\left[\Xi^{6}_{220}(O_1)+0.0808\Xi^{6}_{220}(O_2)\right]\right\}
\end{aligned}
$$

$$
\begin{aligned}
V_{222}^{00}(r) &= \frac{10\sqrt{10\pi}}{\sqrt{7}r^6}\left\{\frac{d_{ON}}{r^6}\left[\Xi_{222}^{12}(O_1)-3.7574\Xi_{222}^{12}(O_2)\right]-e_{ON}\left[\Xi_{222}^{6}(O_1)-3.7574\Xi_{222}^{6}(O_2)\right]\right\}\\
V_{222}^{\pm 20}(r) &= \frac{10\sqrt{15\pi}}{\sqrt{7}r^6}\left\{\frac{d_{ON}}{r^6}\left[\Xi_{222}^{12}(O_1)+0.0808\Xi_{222}^{12}(O_2)\right]-e_{ON}\left[\Xi_{222}^{6}(O_1)+0.0808\Xi_{222}^{6}(O_2)\right]\right\}\\
V_{224}^{00}(r) &= \frac{2\sqrt{70\pi}}{3r^5}Q_{zz}^{O_3}Q_{zz}^{N_2}\\
&- \frac{\sqrt{10\pi}}{\sqrt{7}r^6}\left\{\frac{d_{ON}}{r^6}\left[\Xi_{224}^{12}(O_1)-3.7574\Xi_{224}^{12}(O_2)\right]-e_{ON}\left[\Xi_{224}^{6}(O_1)-3.7574\Xi_{224}^{6}(O_2)\right]\right\}\\
V_{224}^{\pm 20}(r) &= \frac{2\sqrt{35\pi}}{3\sqrt{3}r^5}\left(Q_{xx}^{O_3}-Q_{yy}^{O_3}\right)Q_{zz}^{N_2}\\
&+ \frac{10\sqrt{15\pi}}{\sqrt{7}r^6}\left\{\frac{d_{ON}}{r^6}\left[\Xi_{224}^{12}(O_1)+0.0808\Xi_{224}^{12}(O_2)\right]-e_{ON}\left[\Xi_{224}^{6}(O_1)+0.0808\Xi_{224}^{6}(O_2)\right]\right\}
\end{aligned}
$$

where the notation

$$
\Xi_{l_1 l_2 l}^{n}(O_i)=\sum_{p,q}\left(\frac{r_{1O_i}}{r}\right)^p\left(\frac{r_{2N}}{r}\right)^q\frac{(n+p+q-l-3)!!\,(n+p+q+l-2)!!}{(n-2)!\,(p-l_1)!!\,(p+l_1+1)!!\,(q-l_2)!!\,(q+l_2+1)!!}
$$

is introduced and O_i=O_1 (oxygen atom lying on the molecular z-axis of O_3) or O_i=O_2 (oxygen atoms out of z-axis accounted together). For O_3-O_2 system the d_{ON} and e_{ON} parameters are to be replaced by d_{OO} and e_{OO} (see Table 1).

References

[1] A. Barbe, J.J. Plateaux, S. Bouazza, J.-M. Flaud, and C. Camy-Peyret, J. Quant. Spectrosc. Radiat. Transfer 48 (1992) 599-610.

[2] S. Bouazza, A. Barbe, J. J. Plateaux, L. Rosenmann, J. M. Hartmann, C. Camypeyret, J. M. Flaud and R. R. Gamache, J. Mol. Spectrosc. 157 (1993) 271-289.

[3] A. Barbe, L. Regalia, J. J. Plateaux, P. Von Der Heyden, and X. Thomas, J. Mol. Spectrosc. 180 (1996) 175-182.

[4] S.P. Neshyba, R.R. Gamache, J. Quant. Spectrosc. Radiat. Transfer 50 (1993) 443-453.

[5] J. Buldyreva and L. Nguyen, Phys. Rev. A 77 (2008) 042720.

[6] A. Bykov, N. Lavrentieva and L. Sinitsa, Mol. Phys. 102 (2004) 1706-1712.

[7] B. Labani, J. Bonamy, D. Robert, J.M. Hartmann, and J. Taine, J. Chem. Phys. 84 (1986) 4256-4267.

[8] D. Robert, J. Bonamy, J. Phys. 40 (1979) 923-943.

[9] C.G. Gray and K.E. Gubbins, Theory of molecular fluids, Volume 1: Fundamentals, Clarendon press, Oxford, 1984.

[10] D. Reuter, D.E. Jennings, J.W. Brault, J. Mol. Spectrosc. 115 (1986) 294-304.

[11] G. Herzberg, Spectra of diatomic molecules, Princeton, van Nostrand, 1966.

[12] http://ozone.iao.ru/

[13] S. Michajlenko, private communication.

[14] V.I. Starikov, V.G. Tyuterev, Intramolecular interactions and theoretical methods in spectroscopy of nonrigid molecules, Siberian Branch of Russian Academy of Sciences, Tomsk, 1997 (in Russian).

[15] B.J. Drouin, J. Fischer, R.R. Gamache, J. Quant. Spectrosc. Rad. Transfer 83 (2004) 63-81.

[16] J.O. Hirschfelder, C.F. Curtiss, R.B. Bird, Molecular theory of gases and liquids, New York, Wiley, 1964.

[17] H. Yasuda, T. Yamamoto, Prog. Theor. Phys. 45 (1971) 1458.

[18] W. Gordy, W. V. Smith, and R. F. Trambarulo, Microwave spectroscopy, John Wiley and Sons, London, Chapman and Hall, Ltd, 1953.

[19] P. W. Anderson, Phys. Rev. 76 (1949) 647.

[20] C.J. Tsao and B.Curnutte, J. Quant. Spectrisc. Radiat. Transfer 2 (1961) 41-91.

[21] B. Labani, J. Bonamy, D. Robert, and J.M. Hartmann, J. Chem. Phys. 87 (1987) 2781-2789.

[22] C. Camy-Peyret, A. Valentin, Ch. Claveau, A. Bykov, N. Lavrentieva, V. Saveliev, L. Sinitsa, J. Mol. Spectrosc. 224 (2004) 164-175.

[23] V. Zeninari, B. Parvitte, D. Courtois, N.N. Lavrentieva, Yu. N. Ponomarev, G. Durry, Mol. Phys. 102 (2004) 1697-1706.

[24] S.A. Tashkun, V.I. Perevalov, J.-L. Teffo, A.D. Bykov, N.N. Lavrentieva, CDSD-1000, J. Quant. Spectrosc. Radiat. Transfer 82 (2003) 165-196.

[25] ftp://ftp.iao.ru/pub/CDSD-1000

[26] http://wadis.saga.atmos.iao.ru

[27] A.D. Bykov, N.N. Lavrentieva, T.P. Mishina, L.N. Sinitsa, R.J. Barber, R.N. Tolchenov, J. Tennyson, J. Quant. Spectrosc. Radiat. Transfer 109 (2008) 1834-1844.

[28] J.T. Hodges, D. Lisak, N. Lavrentieva, A. Bykov, L. Sinitsa, J. Tennyson, R.J. Barber, R.N. Tolchenov, J. Mol. Spectrosc. 249 (2008) 86-94.

[29] A.D. Bykov, N.N. Lavrentieva, T.M. Petrova, L.N. Sinitsa, A.M. Solodov, R.J. Barber, J. Tennyson, R.N. Tolchenov, Optika i spectroscop. 105 (2008) 25-31.

[30] N. Lavrentieva, A. Osipova, L. Sinitsa, C. Claveau, A. Valentin, Mol. Phys. 106 (2008) 1261-1266.

[31] R.P. Leavitt, J. Chem. Phys. 73 (1980) 5432-5450.

[32] J.M.Flaud, C. Camy-Peyret, V. Malathy Devi, C.P. Rinsland, M.A.H. Smith, J. Mol. Spectrosc. 124 (1987) 209-217.

Table 1: Physical parameters characterizing the intermolecular potential O_3-$N_2(O_2)$ [2].

d_{ij} $(10^{-7} erg\ \mathring{A}^{12})$	e_{ij} $(10^{-10} erg\ \mathring{A}^{6})$	$\lvert r_{1i}\rvert, \lvert r_{2j}\rvert$ $(\mathring{A})$	Q $(10^{-26} esu)$
$d_{ON} = 0.392$	$e_{ON} = 0.319$	$\lvert r_{1O_1}\rvert = 0.446$	$\mu_x(O_3) = 0.532D$
$d_{OO} = 0.239$	$e_{OO} = 0.276$	$\lvert r_{1O_2}\rvert = 1.111$	$Q_{xx}(O_3) = -0.7$
		$\lvert r_{2N}\rvert = 0.549$	$Q_{yy}(O_3) = 2.1$
		$\lvert r_{2O}\rvert = 0.604$	$Q_{zz}(O_3) = -1.4$
			$Q(N2) = -1.3$

Figure captions

Figure 1. Molecular frame for the active ozone molecule.

Figure 2. Semiclassical RBE and semiempirical SE line widths in comparison with experimental and semiclassical RB values [2] for the Q-branch of $\nu_1 + \nu_3$ vibrational band of ozone perturbed by nitrogen (a) and oxygen (b).

Figure 3. Comparison of semiempirical line widths with experimental [2, 3] and theoretical RB [2] values for P-branch of O_3-N_2 $\nu_1 + \nu_3$ band.

Figure 4. Influence of a separate small-middle-high J-values fitting for c_1, c_2 parameters of the semiempirical approach (P- and R-branches used simultaneously) for O_3-N_2 (a) and O_3-O_2 (b) systems.

Figure 5. Rotational J-dependence of O_3-N_2 $\nu_1 + \nu_3$ line widths for two "families" of lines from R-branch: $J+1\ 0\ J+1 \leftarrow J\ 0\ J$ (a) and $J+1\ 2\ J-1 \leftarrow J\ 2\ J-2$ (b).

Figure 6. Line width dependence on the quantum number K_a for low ($J = 4$, a) and high ($J = 24$, b) rotational quantum number values in the R-branch of O_3-N_2 $\nu_1 + \nu_3$ band.